Coherent control of multiphoton-ionization passage of excited-state rubidium atoms

Sangkyung Lee,[1,2] Han-gyeol Lee,[1] Junwoo Cho,[1] Jongseok Lim,[1] Chang Yong Park,[2] and Jaewook Ahn[1,*]

[1]*Department of Physics, KAIST, Daejeon 305-701, Korea*

[2]*Korea Research Institute of Science and Standards, Daejeon 305-340, Korea*

(Received 1 May 2012; published 31 October 2012)

We have investigated multiphoton-ionization passages of rubidium atoms initiated from the excited $5P_{3/2}$ energy state. For this we used coherent control schemes based on femtosecond laser pulse shaping applied to cold atoms spatially isolated in a magneto-optical trap. With programed laser pulses of spectral π-phase step, of which location was varied within the laser spectrum, the sequential two-photon-ionization passage along the $5P_{3/2}$-$5D$ continuum was probed in terms of trap-loss spectroscopy. The coherent control two-photon-ionization method unveiled not only the resonantly enhanced two-photon ionization but also the asymmetric nature of the ionization profile structure given as a function of the spectral phase step location. Experimental results show good agreement with the second-order perturbation calculation of the constituent possible ionization passages.

DOI: 10.1103/PhysRevA.86.045402 PACS number(s): 32.80.Qk, 32.80.Wr, 42.65.Re, 37.10.De

Development of ultrafast coherent control has opened new possibilities towards manipulation of the quantum dynamics of atoms and molecules [1]. With the use of programed pulse shapes, one can coherently control atomic or molecular processes by steering them through desirable quantum passages. This novel concept of ultrafast coherent control has been applied to, for example, the optimization of nonlinear processes, selective chemical photodissociations, advanced spectroscopy, and quantum computing [1–3]. In particular, ultrafast coherent control in multiphoton absorption has been studied widely with alkali-metal atoms, such as cesium, rubidium, and sodium [4–6], in which studies the quantum interference among multiple degenerate quantum passages has been probed by laser spectral phase shaping. Previous studies have been mainly focused on the multiphoton absorption transitions between discrete electronic energy states [7–12] or the multiphoton ionization between resonant and nonresonant multiphoton passages to ionization [13–15]. However, when we consider an ionization process involved with a multiphoton process where the final state is an unbound continuum state, the coherent control schemes based on discrete-state quantum interference need to be revised: Incoherent summation of multiphoton ionization probability distribution in the final state continuum is required. To further explore the coherent control of multiphoton ionization processes, one could consider femtosecond laser pulse shaping with shape parameters, such as chirp, phase step, and phase modulation.

In this paper, we consider two-photon-ionization passages of rubidium (Rb) atoms in the excited $5P_{3/2}$ energy state. For this, we use ^{85}Rb atoms captured in a magneto-optical trap (MOT). Cold atoms in a MOT enable facile observation of the given two-photon transitions initiated from the excited state of the optical cycling transition. Moreover, the fluorescence measurement of the cooling transition provides an indirect probing tool for the weak transitions in terms of trap-loss spectroscopy [16,17]. In general, translational motions of atoms cooled in a MOT are so weakened that external effects such as Doppler broadening and collisional shifts which might disturb optical measurements involved with the internal states of atoms and molecules are suppressed, which feature has made various precision spectroscopies of atoms and molecules possible in conjunction with the frequency comb technique [18,19]. Also, there have been attempts to use cold atoms for atomic photoassociation processes towards diatomic molecular formation [17,20], and for studies of vibrational wave-packet dynamics of cold molecules [21].

Let us consider the two-photon ionization of an atom from an initial state $|i\rangle$ to a continuum state $|\vec{k}\rangle$, via an intermediate state $|m\rangle$, which is induced by a weak femtosecond laser pulse with an electric field $E(t)$. The second-order perturbation theory predicts that the two-photon transition probability amplitude, denoted by $\psi_{\vec{k}i}$, is given by

$$\psi_{\vec{k}i} = -\frac{1}{i\hbar^2}\sum_m \mu_{\vec{k}m}\mu_{mi}\left[i\pi\,\tilde{E}(\omega_{\vec{k}m})\tilde{E}(\omega_{mi}) + \mathrm{P}\int_{-\infty}^{\infty} d\omega \frac{\tilde{E}(\omega)\tilde{E}(\omega_{\vec{k}i}-\omega)}{(\omega-\omega_{mi})}\right], \quad (1)$$

where $\mu_{\vec{k}m}$ and μ_{mi} are the dipole moments for $|i\rangle \to |m\rangle$ and $|m\rangle \to |\vec{k}\rangle$ transitions, respectively, ω_{mi} and $\omega_{\vec{k}m}$ are their angular frequencies, and $\omega_{\vec{k}i} = \omega_{mi} + \omega_{\vec{k}m}$. P denotes a Cauchi principal value calculation, and the spectral amplitude is given by $\tilde{E}(\omega) = \mathcal{F}[E(t)e^{-i\omega_o t}]$, where ω_o is the mean frequency of the laser field. Then, the total ionization probability Γ is given as the sum of the ionization probabilities to all possible continuum states $|\vec{k}\rangle$, or $\Gamma = \int d^3k|\psi_{\vec{k}i}|^2$, and from the energy conservation $E_i + \hbar\omega_{\vec{k}i} = E_{\mathrm{ion}} + \hbar^2k^2/2m$ with E_i the initial state energy and E_{ion} the energy of the ionization level, and Γ is given by

$$\Gamma = \frac{\sqrt{2m^3}}{\hbar^2}\int_{E_o/\hbar}^{\infty} d\omega_{\vec{k}i}\sqrt{\hbar\omega_{\vec{k}i} - E_o}\int d\Omega_k|\psi_{\vec{k}i}|^2, \quad (2)$$

where E_o is the energy difference between the initial state and the ionization level (i.e., $E_o = E_{\mathrm{ion}} - E_i$), and Ω_k denotes the solid angle in momentum space.

Experiments were performed with a setup illustrated in Fig. 1, which comprised an ultrafast laser amplifier system equipped with pulse-shaping capability, a magneto-optical trap for cold Rb atoms, and a synchronized fluorescence detection

*jwahn@kaist.ac.kr

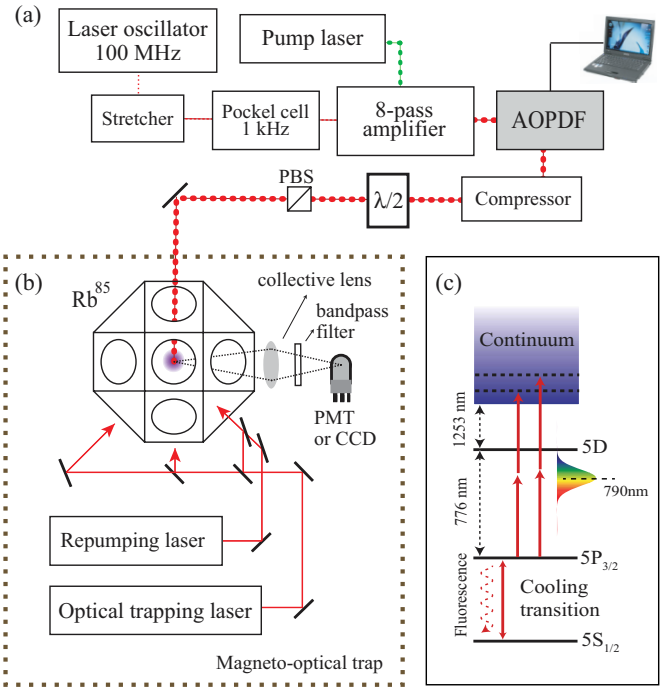

FIG. 1. (Color online) Schematic setup for coherent control experiments of the two-photon ionization of atomic rubidium (Rb^{85}) in the $5P_{3/2}$ state. (a) Generation of shaped ultrafast laser pulses using acousto-optic programmable dispersion filter (AOPDF). (b) Magneto-optical trap for cooling and trapping of Rb atoms. (c) Energy level diagram for the sequential $|5P_{3/2}\rangle$-$|5D\rangle$-|continuum⟩ two-photon-ionization process.

system. The laser system and its pulse-shaping procedure were described in the earlier publications [22–24]. Briefly, femtosecond near-infrared laser pulses of programed spectral amplitude and phase were produced by an acousto-optic dispersive spectral filter [25] as in Fig. 1(a), and the shaped laser pulses of an energy of up to 80 μJ illuminated, being unfocused, over the atom-interaction area of 10^{-1} cm^2, and the pulse repetition rate was 1 kHz. The wavelength center of the laser was located at 790 nm ($\omega_o = 2.4 \times 10^{15}$ rad Hz) and the laser bandwidth was 12–15 nm.

The atomic system was ^{85}Rb atoms captured in a MOT [26] as shown in Fig. 1(b), where the initial state was the excited state, $|i\rangle = |5P_{3/2}\rangle$, and the intermediate state was the $5D$ manifold, or $|m\rangle = |5D\rangle$. As illustrated in the energy level diagram in Fig. 1(c), the atoms initially remained cycling between the $5S_{1/2}$ and $5P_{3/2}$ states. Upon the femtosecond (fs) laser pulse interaction some of the atoms were ionized along the $|5P_{3/2}\rangle$-$|5D\rangle$-|continuum⟩ path, and the others were either unaffected, or first excited to other states but then brought back to the cooling cycle after radiative decay. As the laser repetition rate (1 kHz) was significantly slower than the spontaneous decay rate of the Rb in the $5P_{3/2}$ state, the steady-state fluorescence signal from the $|5S_{1/2}\rangle$-$|5P_{3/2}\rangle$ cycling transition was used to estimate the remaining atom number in the trap, or the ionization probability of the atoms was measured. The fs laser beam was linearly polarized in the horizontal plane and the ionization rate was not sensitive to the initial hyperfine energy levels. The steady-state fluorescence signal from the cold Rb cloud was imaged either onto a photomultiplier tube (PMT) or a charge-coupled device (CCD) camera screen, through a 5-nm spectral interference filter centered at 780-nm wavelength for the $|5P_{3/2}\rangle$-$|5S_{1/2}\rangle$ decay.

The trap-loss dynamics of the experimented light-matter interaction is as follows: As the steady-state atom number is related to the ionization probability in Eq. (2) the number of trapped atoms is governed by a rate equation; when the trapped atoms are illuminated by a train of fs laser pulses, the rate equation for the number of atoms N in both the $5P_{3/2}$ and $5S_{1/2}$ states can be written as

$$\frac{dN}{dt} = \eta - \gamma N - f\Gamma N \sum_{n=0}^{\infty} \delta(t - nt_o), \tag{3}$$

where η and γ are the loading and loss rates of the MOT, respectively, f is the fraction of the number of atoms in the $5P_{3/2}$ state, $\delta(x)$ is the Dirac delta function [27], and t_o is the temporal separation of the fs laser pulses, which is 1 ms. So, the ionization probability in Eq. (2) can be measured from its solution given by

$$\Gamma = \frac{N_o - N_{\rm ss}}{f N_{\rm ss}}(e^{\gamma t_o} - 1), \tag{4}$$

where $N_o = \eta/\gamma$ is the initial atom number and $N_{\rm ss}$ is the atoms number in the steady state. In our experimental condition, $N_o = 10^7$ and $\gamma = 0.35$ Hz. So, by the first-order approximation of γt_o, which is 3.5×10^{-4}, $N_{\rm ss}$ is given as

$$N_{\rm ss}(\Gamma) = \frac{N_o}{1 + f\Gamma/\gamma t_o}. \tag{5}$$

It is noted that in the trap-loss dynamics in Eq. (3) the collisional loss term is ignored, because the excited collision leading the atoms to noncooling states is given by $\beta N_{\rm ss}$ with $\beta \approx 10^{-11}$ Hz [28] and, considering the fact that the density of atoms drops to 7×10^4/cm^3 upon the fs-laser interaction, the excited collision rate is estimated to 7×10^{-7} Hz, considerably smaller than the ionization loss. Also, the radiation pressure loss due to the 780-nm D_2 line resonant spectrum was kept unchanged throughout the experiment.

The coherent control experiment utilized a spectral phase step for the control pulse. Starting with a broadband spectrum initially of a Gaussian pulse $E(t) = E_o \exp(-t^2/\tau^2 + i\omega_o t)$ with a pulse width $\tau = 55$ fs, we programed its amplitude spectral function $\tilde{E}(\omega)$ to have a π-phase spectral step in such a way that the relative phase $\phi(\omega)$ is given as

$$\phi(\omega) = \pi\Theta(\omega - \omega_\pi), \tag{6}$$

where $\Theta(x)$ is the Heaviside step function [27], defined as $\Theta(x) = 0$ for $x < 0$ and $\Theta(x) = 1$ for $x > 0$, and ω_π is the spectral location of the π-phase step. After illuminating such shaped laser pulses 300 times, over a 300-ms time duration, we measured the 780-nm fluorescence signal from the trapped atoms to estimate the number of trapped atoms in the steady state. Such measurement was repeated by varying the ω_π while the energy of the shaped laser pulses was kept constant at 8 μJ.

Figure 2 shows the experimental result. The measured fluorescence data shown with circles are proportional to the number of remaining atoms in the trap. The measured

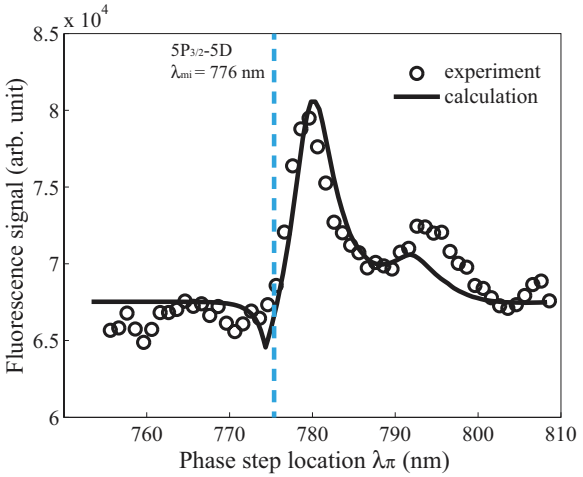

FIG. 2. (Color online) $|5P_{3/2}\rangle$-$|5S\rangle$ fluorescence signal measured as a function of the π-phase step location λ_π from the coherent control ionization experiment described in the text. Experimental measurement (circles) is compared with the calculated number of remaining atoms in the trap (solid line).

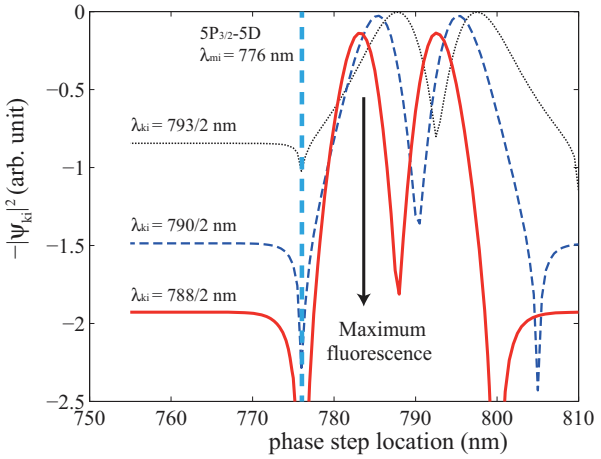

FIG. 3. (Color online) Calculated three-level ladder two-photon transition probability to three continuum states: $\lambda_{ki} = 788/2$ nm (red solid line), $\lambda_{ki} = 790/2$ nm (blue dashed solid), and $\lambda_{ki} = 793/2$ nm (black dotted line). Note that the y axis is the negative probability proportional to the number of remaining atoms in the MOT.

fluorescence was fitted to a function $F = a/(1 + b\Gamma') + c$, where $c = 6.4 \times 10^4$ is the background fluorescence and Γ' is the relative ionization probability. By using the fitted parameters $a = 1.5 \times 10^5$ and $b = 4 \times 10^{-4}$ and the relation $f/\gamma t_o \Gamma = b\Gamma'$ from Eq. (5), the ionization loss rate was extracted as, for example, $\Gamma = 0.036$ Hz for the shaped pulse of $\lambda_\pi = 780$ nm. The result in Fig. 2 shows two features: (1) the two-photon ionization is suppressed in the broad spectral range from $\lambda_\pi = 778$ to 800 nm, where $\lambda_\pi = 2\pi c/\omega_\pi$, and (2) the ionization suppression appears asymmetric with a bigger suppression in the half spectral region near 776 nm. Both features are confirmed by the numerical calculation carried out based on Eqs. (1)–(5), shown with the solid line.

To understand the observed behaviors, we analyze the two-photon-ionization process of the Rb atoms in $|5P_{3/2}\rangle$. The atoms in the trap are under the cycling transition between the $|5S\rangle$ and $|5P_{3/2}\rangle$, allowing both two- and three-photon ionizations. However, for the laser intensity used in the experiment, the three-photon-ionization events from the ground state were experimentally verified as less than 10% of the two-photon-ionization events from the $5P_{3/2}$ state in a series of direct ionization measurements by turning on and off the optical cycling transition. It can be understood as the spatial averaging effect of the nonlinear process: With the MOT volume of 1-mm-diameter sphere and the focused fs beam of 50-μm diameter, the loss rate is spatially averaged from the weak-field to the strong-field regimes. Then, despite $\mu_{km}\mu_{mi}\mu_{ig}E_0^3/\hbar^3 > 1$ (i.e., three-photon ionization), the contribution of $\mu_{km}\mu_{mi}E_0^2/\hbar^2$ (i.e., two-photon ionization) prevails over the contribution of the three-photon ionization because the interaction volume in the perturbative regime ($\mu E_0/\hbar \ll 1$) is much larger than that in the nonperturbative regime. Therefore, the total loss rate is mainly determined by the two-photon ionization. It is also noted that the resonant two-photon transition, the first term in Eq. (1), is relatively unimportant in the performed experimental condition because the spectral density at the laser wavelength of 776 nm resonant to the $|5P_{3/2}\rangle$-$|5D\rangle$ transition was low due to the laser bandwidth. As a result, the main contribution for the experimented ionization comes from the nonresonant two-photon-ionization contribution, the second term in Eq. (1).

In Fig. 3, the calculated (minus) ionization probabilities, $-|\psi_{ki}|^2$, to particular final continuum states $|k\rangle$'s are plotted, where $\mu_{km} = 1.93 \times 10^{-37}$ C m for $\lambda_{km} = 788$ nm is from the photoionization cross-section calculation [29]. In general, the two-photon-ionization probability, for example, the red solid line drawn for the case $\lambda_{ki} = 788/2$ nm, shows a symmetric profile around a sharp local minimal point at the center of the two resonant wavelengths [4]. At the center of the two resonant wavelengths (i.e., $\omega_\pi = \omega_{ki}/2$), the two-photon-ionization probability amplitude is given by $\int_0^{\omega_{ki}/2} |E(\omega)||E(\omega_{ki} - \omega)| \exp[i(\pi/2 - \pi/2)]d\omega + \int_{\omega_{ki}/2}^{\infty} |E(\omega)||E(\omega_{ki} - \omega)| \exp[i(-\pi/2 + \pi/2)]d\omega$. So, all possible two-photon-ionization passages from the $|i\rangle$ state to the $|k\rangle$ state are added totally constructively. However, if $0 < \omega_\pi < \omega_{ki}/2$, it is given that $\int_0^{\omega_\pi} |E(\omega)||E(\omega_{ki} - \omega)|d\omega + \int_{\omega_\pi}^{\omega_{ki}-\omega_\pi} |E(\omega)||E(\omega_{ki} - \omega)| \exp(i\pi)d\omega + \int_{\omega_{ki}-\omega_\pi}^{\infty} |E(\omega)||E(\omega_{ki} - \omega)|d\omega$, or the ionization passages are added partially destructively, because the second term is out of phase with respect to the first and third terms. Moreover, due to the symmetry, the probability amplitude for the region $\omega_{ki}/2 < \omega_\pi < \infty$ is similar to that for $0 < \omega_\pi < \omega_{ki}/2$, which explains the symmetric shape of the two-photon-ionization probability to a particular continuum state as shown in Fig. 3.

When the individual ionization profiles are all added up, however, the net ionization probability profile becomes asymmetric because the symmetric centers of the individual profiles are all different from each other, and the minimum net ionization region, or the maximum fluorescence region, appears larger in the left-half wavelength region near the resonant wavelength of 776 nm as illustrated in Fig. 3. As confirmed by the $|5P_{3/2}\rangle$-$|5S\rangle$ fluorescence signal in Fig. 2, the remaining atom number in the trap shows good agreement

with the (minus) calculated the net two-photon-ionization probability to the continuum energy band. Therefore, we can conclude that the minimum ionization rate is originated from the sum of the destructively interfered two-photon-ionization probabilities, or the origin of the asymmetric ionization profile is due to the two-photon transition contributions to all continuum states, and, thus, the incoherent sum of the transition probabilities has the minimum of the total two-photon transition near the $|5P_{3/2}\rangle$-$|5D\rangle$ resonant wavelength.

In conclusion, we have investigated two-photon-ionization passages of the excited Rb atoms with a coherent control method. In the experiment carried out with ultrafast shaped laser pulses of a π-phase spectral step, the sequential two-photon-ionization passage along $|5P_{3/2}\rangle$-$|5D\rangle$-$|\text{continuum}\rangle$ has been sensitively probed in conjunction with trap-loss spectroscopy. The location of the spectral phase step has unveiled not only the resonantly enhanced two-photon ionization but also the asymmetric ionization profile structure of the incoherent sum of the constituent two-photon-ionization passages to the continuum state despite the symmetric control profiles of ionization passages to individual continuum states. Theoretical analysis based on the second-order perturbation calculation as well as the trap-loss dynamics has confirmed the experimental results.

The authors thank the anonymous referee for valuable comments. This research was supported by Basic Science Research and Mid-career Researcher Programs through the National Research Foundation of Korea (NRF) funded by the Ministry of Education, Science and Technology (2009-0090843 and 2010-0013899).

[1] M. Shapiro and P. Brumer, *Principles of the Quantum Control of Molecular Processes* (Wiley, New York, 2003).
[2] T. Brixner, T. Pfeifer, G. Gerber, M. Wollenhaupt, and T. Baumert, in *Femtosecond Laser Spectroscopy*, edited by P. Hannaford (Kluwer, Dordecht, 2004).
[3] D. Goswami, Phys. Rep. **374**, 385 (2003).
[4] D. Meshulach and Y. Silberberg, Phys. Rev. A **60**, 1287 (1999).
[5] D. Felinto, L. H. Acioli, and S. S. Vianna, Opt. Lett. **25**, 917 (2000).
[6] S. Lee, J. Lim, C. Y. Park, and J. Ahn, Opt. Express **19**, 2266 (2011).
[7] V. Blanchet, C. Nicole, M.-A. Bouchene, and B. Girard, Phys. Rev. Lett. **78**, 2716 (1997).
[8] D. Meshulach and Y. Silberberg, Nature **396**, 239 (1998).
[9] N. Dudovich, D. Oron, and Y. Silberberg, Phys. Rev. Lett. **92**, 103003 (2004).
[10] C. Trallero-Herrero, D. Cardoza, T. C. Weinacht, and J. L. Cohen, Phys. Rev. A **71**, 013423 (2005).
[11] Z. Amitay, A. Gandman, L. Chuntonov, and L. Rybak, Phys. Rev. Lett. **100**, 193002 (2008).
[12] S. Lee, J. Lim, and J. Ahn, Opt. Express **17**, 7648 (2009).
[13] C. Chen, Y.-Y. Yin, and D. S. Elliott, Phys. Rev. Lett. **64**, 507 (1990).
[14] A. Assion, T. Baumert, J. Helbing, V. Seyfried, and G. Gerber, Chem. Phys. Lett. **259**, 488 (1996).
[15] R. R. Jones, Phys. Rev. Lett. **75**, 1491 (1995).
[16] O. Maragó, D. Ciampini, F. Fuso, E. Arimondo, C. Gabbanini, and S. T. Manson, Phys. Rev. A **57**, R4110 (1998).
[17] W. Salzmann, T. Mullins, J. Eng, M. Albert, R. Wester, M. Weidemüller, A. Merli, S. M. Weber, F. Sauer, M. Plewicki, F. Weise, L. Wöste, and A. Lindinger, Phys. Rev. Lett. **100**, 233003 (2008).
[18] M. C. Stowe, A. Pe'er, and J. Ye, Phys. Rev. Lett. **100**, 203001 (2008).
[19] T. H. Yoon, A. Marian, J. L. Hall, and J. Ye, Phys. Rev. A **63**, 011402(R) (2000).
[20] W. Salzmann, U. Poschinger, R. Wester, M. Weidemüller, A. Merli, S. M. Weber, F. Sauer, M. Plewicki, F. Weise, A. M. Esparza, L. Wöste, and A. Lindinger, Phys. Rev. A **73**, 023414 (2006).
[21] M. Viteau, A. Chotia, M. Allegrini, N. Bouloufa, O. Dulieu, D. Comparat, and P. Pillet, Science **321**, 232 (2008).
[22] S. Lee, J. Lim, J. Ahn, V. Hakobyan, and S. Guerin, Phys. Rev. A **82**, 023408 (2010).
[23] J. Lim, H. G. Lee, J. U. Kim, S. Lee, and J. Ahn, Phys. Rev. A **83**, 053429 (2011).
[24] J. Lim, H. G. Lee, S. Lee, and J. Ahn, Phys. Rev. A **84**, 013425 (2011).
[25] F. Verluise, V. Laude, Z. Cheng, Ch. Spielmann, and P. Tournois, Opt. Lett. **25**, 575 (2000).
[26] W. D. Phillips, Rev. Mod. Phys. **70**, 721 (1998).
[27] G. B. Arfken and H. J. Weber, *Mathematical Methods for Physicists,* 5th ed. (Academic, New York, 2000).
[28] D. Hoffmann, P. Feng, R. S. Williamson, and T. Walker, Phys. Rev. Lett. **69**, 753 (1992).
[29] B. C. Duncan, V. Sanchez-Villicana, P. L. Gould, and H. R. Sadeghpour, Phys. Rev. A **63**, 043411 (2001).